Adsorption 5, 245–259 (1999)

Analysis of Equilibrium PSA Performance with an Analytical Solution

JONG-HO PARK* AND JONG-DUK KIM
Department of Chemical Engineering, KAIST, 373-1, Kusungdong, Yusungku, Taejon, Korea

JONG-NAM KIM AND SOON-HAENG CHO†
Korea Institute of Energy Research, 71-2, Jangdong, Yusungku, Taejon, Korea

Received March 9, 1998; Accepted August 3, 1998

Abstract. Five-step PSA cycles consisting of pressurization with product, adsorption, co-current depressurization, blowdown, and purge steps have been analyzed with equilibrium model assuming uncoupled linear isotherms and isothermal condition. Unlike the previous models, the proposed model is not restricted to the operating conditions that ensure a complete shock transition of concentration profile at the end of the high pressure adsorption step. The operating conditions could have two classifications: one is utilizing the column completely before blowdown, and the other is not. As the selectivity increases, it is more difficult to utilize the column completely before the blowdown step. There is an optimum co-current depressurization pressure which maximizes the recovery at the given extent of purge. The optimum co-current depressurization pressure decreases as the purge quantity decreases. On the less selective adsorbent, the recovery at the optimum co-current depressurization pressure increases with the decrease of purge quantity without much sacrifice of the throughput. But, on the highly selective adsorbent, there is an extent of purge and corresponding value of cocurrent depressurization pressure below which the recovery is not greatly improved while the throughput decreases rapidly, which limits the number of pressure equalization steps can be included.

Keywords: pressure swing adsorption, equilibrium model, analytical solution, optimum co-current depressurization pressure

1. Introduction

Pressure swing adsorption (PSA) is used in many industrial applications ranging from the separation of a gaseous mixture into its components to the purification of an inert carrier gas by the elimination of impurities. A PSA process usually involves a series of adsorption beds, each executing the same sequence of operations but shifted in phase. The basic operations that are performed on each bed include pressurization, high pressure adsorption, blowdown, and purge. In addition to the basic operations, pressure equalization steps are often involved in multi-bed PSA processes. The performance of a PSA process is determined by operating conditions of all of these involved steps in a complicated manner. For the PSA process based on the different equilibrium selectivities of the components in the gas mixture, the solution derived by the local equilibrium model can predict the PSA performance relatively easily.

The first equilibrium model for the ideal dilute system was developed by Shendalam and Mitchell (1972). Fernandez and Kenney (1983) later extended the theory to the separation of bulk binary mixture with linear isotherms and paid particular attention to the pressurization, but resorted to numerical integration of the relevant equations. Analytical solutions to the equations governing PSA processes for an arbitrary feed composition were subsequently developed (Knaebel and Hill, 1985) for complete purge and uncoupled linear

*Present address: Korea Institute of Energy Research, A1-2 Jangdong, Yusungku, Taejon, Korea.
†To whom correspondence should be addressed.

isotherms. They have proved that pressurization with product (a backfill step) gives better light component recovery than pressurization with the feed mixture. A complete purge is not always necessary when a large fraction of the feed mixture is the heavy component. The effect of incomplete purge has been treated by the studies of Matz and Knaebel (1988). They concluded that incomplete purge gives better light component recovery, not identifying the optimum purge condition by a general formula. The optimum purge condition has been investigated by Rousar and Ditl (1993). In their analysis, the column was assumed to be saturated with feed composition at the end of the high pressure adsorption step, which could only be true for some special cycles. The process cycles considered by the above models were four-step PSA cycles including only the basic operations.

The first analysis of the PSA process including the co-current depressurization step has been made by Suh and Wankat (1989). They reported that there is an optimum co-current depressurization pressure which maximizes the light product recovery. Bossy et al. (1992) also mentioned the existence of optimum co-current depressurization pressure even when the isotherm is nonlinear. Both of them assumed that a bed was completely regenerated after the purge step. Consequently, they could not understand the relation between optimum co-current depressurization pressure and incomplete purge.

More general PSA cycles which accommodate incomplete purge and co-current depressurization have been analyzed by Chiang (1995). He discussed the optimal purge and feed amount which maximize the recovery. Subsequently, he compared several cycle schemes in terms of light component recovery and throughput, and gave an explicit expression between optimum feed and purge amount (Chiang, 1996). He assumed that a complete shock formed at the end of the high pressure adsorption step. Thus, the result is limited to the separation of bulk binary mixture by the less selective adsorbent. For the highly selective adsorbent, formation of a complete shock at the end of the high pressure adsorption step is guaranteed when the purge amount is large or feed composition of the heavy component is high, which is not always satisfied in the practical PSA processes.

In this study, the performance characteristics of the five-step PSA cycles will be investigated in a broader range of operating conditions than that of the prior models treated, relaxing the assumption that a complete shock forms at the end of the high pressure adsorption step. Since both the incomplete purge and co-current depressurization steps can enhance the light component recovery, we will examine the effect of these steps on the process performance.

2. Mathematical Model

The mathematical model employed here is basically the same as that proposed by Knaebel and Hill (1985) and Chiang (1996). The notation and relevant equations of their works have been kept unchanged as much as possible to facilitate discussion. The mathematical model is based on the following assumptions: local equilibrium is established, the temperature is constant, axial dispersion is negligible, plug flow conditions are assumed, pressure drop along the column is negligible and gas behavior is ideal. The material balance for component A and the total material balance in a binary mixture can be expressed as follows:

$$\varepsilon\left(\frac{\partial p_A}{\partial t}+\frac{\partial u p_A}{\partial z}\right)+RT(1-\varepsilon)\frac{\partial n_A}{\partial t}=0 \quad (1)$$

$$\varepsilon\left(\frac{\partial P}{\partial t}+\frac{\partial u P}{\partial z}\right)+RT(1-\varepsilon)\frac{\partial n}{\partial t}=0 \quad (2)$$

Where p_A is the partial pressure of the stronger adsorbed component A. P is the total pressure, u is the interstitial velocity, ε is the interstitial bed voidage, n_A is the mole of A adsorbed per unit adsorbent volume, and n represents the total moles adsorbed per unit adsorbent volume. When the isotherms of both components are linear, the adsorbed amount is expressed as

$$n = n_A + n_B = (k_A p_A + k_B p_B)/RT \quad (3)$$

After the elimination of $\partial u/\partial z$, these material balances can be cast into two ordinary differential equations using the method of characteristics:

$$\frac{dz}{dt} = \frac{\beta_A u}{1+(\beta-1)y} \quad (4)$$

$$\frac{dy}{dP} = \frac{(\beta-1)(1-y)y}{[1+(\beta-1)y]P} \quad (5)$$

$$\beta_A = 1/[1+(1-\varepsilon)k_A/\varepsilon], \quad \beta=\beta_A/\beta_B \quad (6)$$

where y is the mole fraction of component A. Equation (4) defines characteristic trajectories in z-t plane and Eq. (5) defines the composition change along the corresponding characteristic trajectories according to the pressure. Since $\beta_A < \beta_B$, β is always less than 1. The small value of β means that the selectivity is high. To solve for the interstitial velocity in the column, one can

eliminate the term $\partial y/\partial t$ from the initial system of the equations, and integrate over the length of the column. Closed solution can be obtained under two conditions:

(a) If $u = 0$ at $z = 0$

$$u = \frac{-z}{\beta_B[1 + (\beta - 1)y]} \frac{1}{P} \frac{dP}{dt} \tag{7}$$

(b) If $dP/dt = 0$

$$\frac{u_1}{u_2} = \frac{1 + (\beta - 1)y_2}{1 + (\beta - 1)y_1} \tag{8}$$

The subscripts 1 and 2 represent the different positions within the column. The above solution is correct when the concentration profile in the bed is continuous. Since the characteristic velocity depends on the composition, the concentration profile may converge or diverge. When the characteristic velocity of the rear of the concentration profile is higher than that of the front, a shock wave develops in the column. If a shock wave forms, the moving velocity of this shock wave is

(a) If $dP/dt \neq 0$

$$u_s = \left.\frac{dz}{dt}\right|_s = \beta_A \frac{u_2 y_2 - u_1 y_1}{y_2 - y_1} = \frac{-\beta z}{[1 + (\beta - 1)y_1][1 + (\beta - 1)y_2]} \frac{1}{P} \frac{dP}{dt} \tag{9}$$

(b) If $dP/dt = 0$

$$u_s = \left.\frac{dz}{dt}\right|_s = \beta_A \frac{u_2 y_2 - u_1 y_1}{y_2 - y_1} = \frac{\beta_A u_2}{1 + (\beta - 1)y_1} = \frac{\beta_A u_1}{1 + (\beta - 1)y_2} \tag{10}$$

where subscripts 1 and 2 represent the rear and front of a shock.

3. Cycle Analysis

The PSA cycle considered is a single column five-step PSA cycle. It consists of: (i) pressurization with product (backfill step), (ii) high pressure adsorption, (iii) co-current depressurization, (iv) countercurrent blowdown, and (v) the purge steps. The feed pressurization step is excluded because it reduces the light component recovery (Knaebel and Hill, 1985). It is assumed that only the pure light component is produced in this cycle. The five-step PSA process could be used to investigate the characteristics of a multi-bed PSA process. The co-current depressurization step can simulate the pressure equalization step and the step providing purge gas in the multi-bed H_2 purification process (Yang, 1987). It should be pointed out that the co-current depressurization pressure can be freely set in the single column PSA process, but it is restricted by both the number of pressure equalization steps and the extent of purge in the multi-bed PSA process. If a co-current depressurization pressure is specified, it always could be achieved in the multi-bed PSA process by adjusting the number of pressure equalization steps and the extent of purge when the effluent of the co-current depressurization step is used to purge the other column (Chiang, 1988). In this regards, to specify the co-current depressurization pressure is the first step to design or schedule a multi-bed PSA process.

3.1. *Blowdown from P_M to P_L*

We begin the analysis from the blowdown step with an assumption that a column is in a uniform gas phase composition of y_M at a pressure P_M after the co-current depressurization step. The assumption is valid in limited operating conditions. If the regeneration is insufficient, the heavy component breaks through the column at the co-current depressurization step before the concentration profile of it develops to a complete shock. This case will be treated later. If the column has a uniform gas phase composition before the blowdown step, the final gas phase composition at the end of the blowdown step also has a uniform composition. The composition of heavy component can be obtained by integrating Eq. (5).

$$\frac{y_b}{y_M} = \left(\frac{1 - y_b}{1 - y_M}\right)^{\beta} \Psi_M^{1-\beta} \tag{11}$$

the y_M and Ψ_M will be identified when a complete analysis of the cycle is made.

3.2. *Product Purge at P_L*

The amount of pure component B needed to purge the column completely is just ϕ. Following the prior works (Knaebel and Hill, 1985; Chiang, 1996), we will let the actual purge quantity be

$$N_{PU} = X \cdot \phi \tag{12}$$

where X is called as the extent of purge. The dimensionless variables such as ϕ, Ψ are the same as defined by Knaebel and Hill (1985). The composition of $y = 0$ will be located at $L(1 - X)$ at the end of the purge step. The minimum extent of purge which pushes the compositon of $y = 0$ out of the feed end is $X_{\min} = [1 + (\beta - 1)y_b]^2$ when the concentration profile after the blowdown step is uniform (Chiang, 1996). If the concentration profile after the blowdown step is not uniform, the minimum extent of purge would be smaller than the value given by the above equation. Even though it is possible to operate a process below the minimum extent of purge at some combination of operating conditions, our analysis will be performed in the range $X \geq [1+(\beta-1)y_b]^2$ for simplicity, which is sufficient to investigate the characteristics of the five-step PSA cycle often encountered in practice. The moles of component A that remains in the column after purge, ϕW_A, is (Chiang, 1996).

$$\phi W_A = \frac{\phi(1 - \sqrt{X})^2}{1 - \beta} \tag{13}$$

3.3. *Backfill Step*

The amount of product gas needed to pressurize a column from P_L to pressure P_H is

$$N_{BF} = \phi\beta(\Psi_H - 1) \tag{14}$$

The displacement of characteristics during the pressure changing step is given by

$$\frac{d \ln z}{d \ln P} = \frac{-\beta}{[1 + (\beta - 1)y]^2} \tag{15}$$

So, the position of the composition $y = 0$ after the backfill step is

$$z|_{y=0} = L(1 - X)\Psi_H^{-\beta} \tag{16}$$

3.4. *High Pressure Adsorption and Co-Current Depressurization Steps*

We will let the amount of feed introduced during the high pressure adsorption step be

$$N_H = \alpha\Psi_H\phi \tag{17}$$

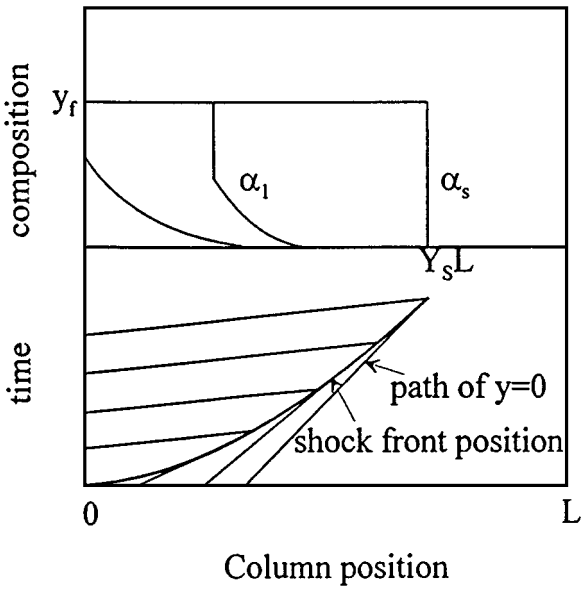

Figure 1. The movement of concentration wave and the characteristic paths during high pressure adsorption step when $Y_S \leq 1$.

α means the fractional utilization of the adsorption column. Only if the column is regenerated completely at the end of purge step, α could be 1. The corresponding amount of light component produced is shown as

$$N_{HP} = \alpha\Psi_H\phi[1 + (\beta - 1)y_f] \tag{18}$$

During the high pressure adsorption step, a concentration shock develops in the column. Figure 1 schematically shows the concentration wave movement and characteristic paths during this step. As the amount of feed increases, a complete shock between $y = 0$ and y_f appears. The amount of feed, α_S, at which a complete shock develops first can be found from material balance for component A and the position of $y = 0$ with amount of feed introduced (Chiang, 1996). Denoting the position where a complete shock forms first as $Y_S L$, the material balance for component A and the position of composition of $y = 0$ are represented as

$$Y_S\phi\Psi_H y_f = \phi W_A + \phi\Psi_H y_f \alpha \tag{19}$$

$$z|_{y=0} = L\left[(1 - X)\Psi_H^{-\beta} + (1 + (\beta - 1)y_f)\alpha\right] \tag{20}$$

Denoting the fractional utilization of a bed when a complete shock develops as α_S, α_S can be found in Eqs. (19)

and (20).

$$\alpha_S = \frac{(1-X)\Psi_H^{1-\beta} y_f (1-\beta) - (1-\sqrt{X})^2}{(1-\beta)^2 y_f^2 \Psi_H} \quad (21)$$

and the corresponding position of a complete shock is obtained from Eq. (19) by substituting Eq. (21) for α. If $Y_S > 1$, a complete shock never forms at the high pressure adsorption step. On the other hand, if $Y_S \leq 1$, a complete shock develops in the column at the high pressure adsorption step at $\alpha \geq \alpha_S$. The value of Y_S is determined by the extent of purge at the given values of y_f, β, and Ψ_H. Thus, the extent of purge determines whether a complete shock develops at the high pressure adsorption step at the given values of y_f, β, and Ψ_H. A critical extent of purge, X_c, could be defined as a minimum extent of purge which ensures a complete shock at the high pressure adsorption step. Although the extent of purge is sufficient to give a complete shock concentration profile at the high pressure adsorption step, it is fulfilled when the fractional utilization of the column exceeds α_S as shown in Fig. 1. All the analytical solutions obtained so far have assumed that the concentration profile had a complete shock transition at the end of the high pressure adsorption step. Thus, prior models can predict the performance of PSA cycles only when the extent of purge and fractional utilization of a column are not less than X_c and α_S, respectively. But, in the practical process, they are not always satisfied. As the selectivity becomes better, the critical extent of purge increases. Thus, to satisfy the condition $X \geq X_c$, too large quantity of product has to be consumed as purge gas. Although the condition, $X \geq X_c$, is satisfied by introducing a lot of purge gas, the concentration profile may not have a complete shock transition at the end of the high pressure adsorption step if one reduces the amount of feed introduced during the high pressure adsorption step in order to increase the moles of the light component produced at the co-current depressurization step and reduce the blowdown loss. When the extent of purge is X_c, a complete shock first forms at the product end during the high pressure adsorption step. Therefore, the light component cannot be produced during the co-current depressurization step and consequently the blowdown loss is significant if one adheres to a complete shock concentration profile at the high pressure adsorption step. But, if one reduces the amount of feed, one can diminish the blowdown loss of the light component since the co-current depressurization step can be conducted. Even when the extent of purge is larger than X_c, the amount of light component produced during the co-current depressurization step is limited if one adheres to a complete shock concentration profile at the high pressure adsorption step. In order to recover more light component at the co-current depressurization step and reduce the blowdown loss, the amount of feed introduced during the high pressure adsorption step has to be adjusted so that the heavy component does not break through the column with the decrease of pressure, even though that makes the concentration profile non-uniform at the end of the high pressure adsorption step.

The movement of the concentration wave and the characteristic paths during the co-current depressurization are schematically shown in Fig. 2 when the concentration profile does not develop to a complete shock at the end of the high pressure adsorption step. In the course of depressurizing co-currently, the initial discontinuous concentration profile never disappears and overtakes the advance wave front, and eventually develops to a complete shock as shown in Fig. 2. If a complete shock forms during the co-current depressurization step, one can find the location and pressure to make the concentration profile has a complete shock by using the material balance for component A and the position of composition $y = 0$ with the decrease of pressure. When a complete shock forms, the material

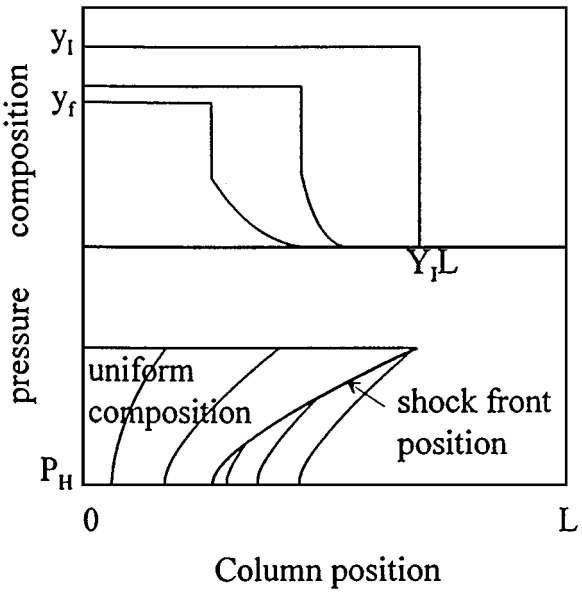

Figure 2. The schematic diagram representing the movement of concentration wave and the characteristic paths during co-current depressurization when $\alpha < \alpha_S$, $Y_I \leq 1$.

balance for component A gives

$$Y_I \phi \Psi_I y_I = \phi W_A + \phi \Psi_H y_f \alpha \tag{22}$$

where Y_I is the dimensionless position at which complete shock forms during the co-current depressurization step. The displacement of $y = 0$ in the course of depressurizing the column is obtained by integrating Eq. (15)

$$z|_{y=0} = L\left[(1-X)\Psi_H^{-\beta} + (1+(\beta-1)y_f)\alpha\right]\left(\frac{\Psi_I}{\Psi_H}\right)^{-\beta} \tag{23}$$

During the pressure changing step, the concentration and the pressure are governed by Eq. (5). Integrating it gives,

$$\Psi_I^{\beta-1} = \left(\frac{y_I}{y_f}\right)\left(\frac{1-y_I}{1-y_f}\right)^{-\beta}\Psi_H^{\beta-1} \tag{24}$$

Inserting Eqs. (23) and (24) to Eq. (22) gives

$$(1-y_I)^\beta = \frac{W_A + \Psi_H \alpha y_f}{(1-X) + (1+(\beta-1)y_f)\Psi_H^\beta \alpha} \times \frac{(1-y_f)^\beta}{y_f}\Psi_H^{\beta-1} \tag{25}$$

From Eqs. (22), (24), and (25), the position where a complete shock first forms during co-current depressurization can be determined. If Y_I is larger than 1, a complete shock never appears during the co-current depressurization step. On the other hand, if $Y_I \leq 1$, a complete shock appears in the column during the co-current depressurization step.

All the concentration profiles appearing at the high pressure adsorption and the co-current depressurization steps could be classified into 5 cases as shown in Fig. 3 according to the value of Y_S and Y_I. A complete shock forms at the high pressure adsorption step if a sufficient

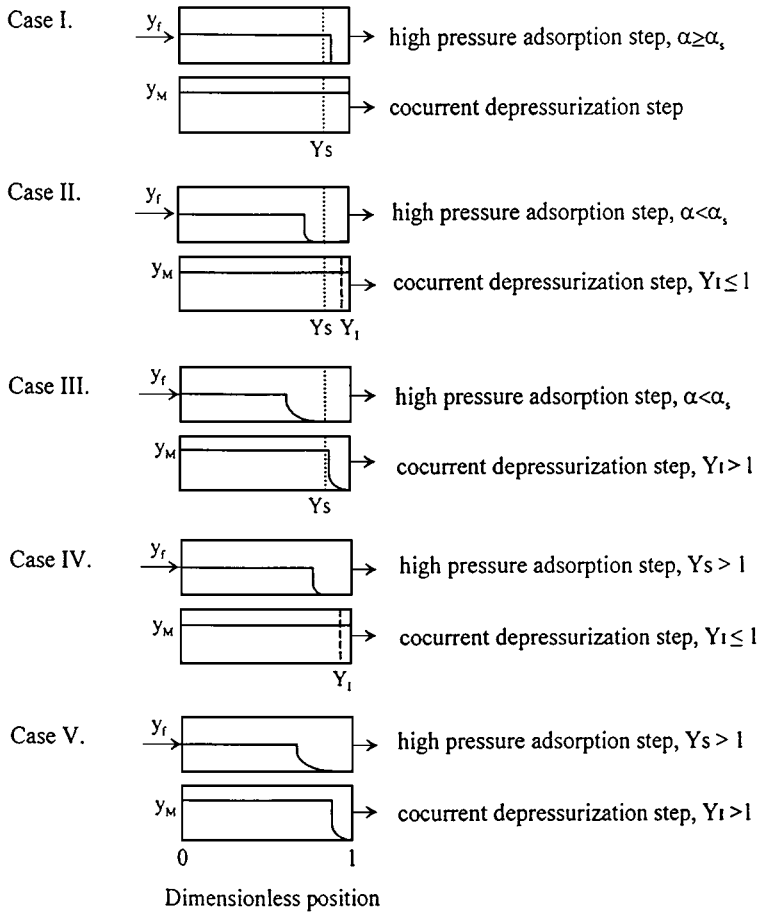

Figure 3. Five cases of concentration profile which arise at the end of high pressure adsorption and co-current depressurization steps.

amount of feed is introduced in Cases I, II, and III, but, not in Cases IV and V. In Cases II and IV, a complete shock first appears during the co-current depressurization step. Cases III and V never have a complete shock during the cycle, which does not meet the assumption: the uniform concentration profile before the blowdown step. For the individual case, the moles of light component produced during the co-current depressurization step is as follows

$$N_{CD} = \phi\beta(\Psi_H - \Psi_M) \tag{26}$$

By deciding the pressure to which the total pressure could be reduced without a breakthrough of the heavy component, we can get the expression for the performance of the five-step PSA cycle.

Case I. A complete shock forms after the high pressure adsorption step and this is the case considered by Chiang (1996). This occurs when $\alpha_S \leq \alpha \leq 1 - W_A/\Psi_H y_f$ and $X \geq X_c$. The dimensionless position of the complete shock, Y, after the high pressure adsorption step could be obtained from the material balance for component A.

$$Y = \alpha + W_A/\Psi_H y_f \tag{27}$$

At the subsequent co-current depressurization step, the shock never disappears and moves to product end. When the shock arrives at the product end, the co-current depressurization step should be stopped to recover the pure light component. From the material balance for component A, we have the following relation

$$\frac{\Psi_M}{\Psi_H} = \frac{Y y_f}{y_M} \tag{28}$$

The composition change during the pressure changing step follows Eq. (5). By solving the equations, the co-current depressurization pressure at which the complete shock reaches the product end can be found

$$\frac{\Psi_M}{\Psi_H} = Y y_f + Y^{1/\beta}(1 - y_f) \tag{29}$$

It is noted from Eq. (29) that Ψ_M is determined by the position of the complete shock after the high pressure adsorption step. That is to say, the amount of light component produced during the co-current depressurization step is related to the amount of feed introduced during the high pressure adsorption step and the extent of purge. Reducing the amount of feed at the constant extent of purge, one can get a greater amount of light component during the co-current depressurization step.

Case II. This occurs when $Y_S \leq 1$ and $\alpha < \alpha_S$. Because Y_I is not larger than 1, a complete shock forms within the column at pressure Ψ_I. In this case, further co-current depressurization can be performed to recover valuable light component like Case I. The lowest co-current depressurization pressure ensuring pure light component product is given similarly to Eq. (29)

$$\frac{\Psi_M}{\Psi_I} = Y_I y_I + Y_I^{1/\beta}(1 - y_I) \tag{30}$$

Case III. This also occurs when $Y_S \leq 1$ and $\alpha < \alpha_S$. But, because $Y_I > 1$, the heavy component breaks through the column before it makes a complete shock. Therefore, to recover the pure light component as product, the co-current depressurization step has to be stopped when the composition of $y = 0$ arrives at the product end. The co-current depressurization pressure at which the composition of $y = 0$ reaches the product end is obtained by equating $z|_{y=0} = L$ from Eq. (23).

$$\Psi_M = \left[(1 - X)\Psi_H^{-\beta} + \{1 + (\beta - 1)y_f\}\alpha\right]^{1/\beta}\Psi_H \tag{31}$$

The gas phase composition at the end of the co-current depressurization step can be obtained by integrating the characteristic equations. But, that is not necessary for our purpose. It is obvious that the concentration profile does not match to the initial condition for the blowdown step assumed: uniform gas phase composition in the column (see Section 3.1). Therefore, to know the process performance of this case, more number of cycle have to be analyzed with the given extent of purge and amount of feed until the concentration profiles at each step approaches the cyclic steady state.

We will analyze the second cycle and extend it to the whole cycle. After the first cycle has been finished, we have the concentration profile at the end of the co-current depressurization step as schematically shown in Fig. 4. During the blowdown step at the second cycle, the position of composition $y = 0$ does not change because the characteristic velocity is zero there. After the purge step, the composition of $y = 0$ will be located at $L(1 - X)$ at a fixed extent

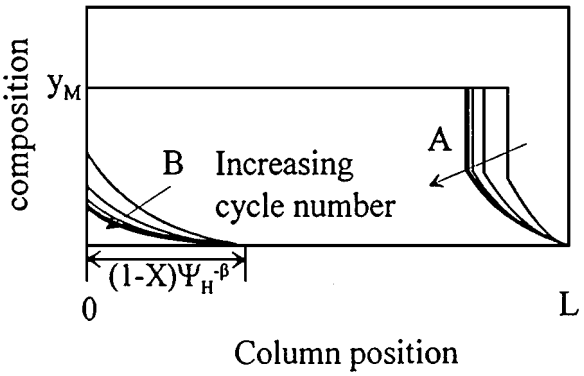

Figure 4. The schematic diagram showing concentration profiles: (a) at the end of the co-current depressurization step and (b) at the end of backfill step with the cycle number when $\alpha < \alpha_S$, $Y_I > 1$.

of purge, X, because characteristic velocity and initial position of composition of $y = 0$ are the same as those at the first cycle. Except the composition of $y = 0$, all the other composition shifts to feed end compared to the first cycle because the initial position of those are closer to the feed end at the second cycle than at the first cycle. Consequently, the composition at fixed position of the column after the blowdown and purge steps is lower than that of the first cycle. When the backfill step is finished, the position of composition of $y = 0$ is given by Eq. (16), i.e., the same as that at the first cycle. The moles needed to backfill the column is also the same as the first cycle and given by Eq. (14) regardless of the concentration profile. The position of the composition $y = 0$ at the end of the high pressure adsorption is also the same as that at the first cycle since the characteristic velocity and the initial position are the same as the first cycle. On the other hand, the position of a shock developing during the high pressure adsorption step shifts to the feed end because the average velocity of the shock front is lower than those at the first cycle. In other words, a complete shock does not develop at the second cycle if the operating conditions are fixed. The light component produced during this step is given by Eq. (18), i.e., the same as the first cycle. If the pressure is reduced to P_M, the composition of $y = 0$ will just arrive at the product end and the composition at the fixed position of the column is lower than that of the first cycle. The moles of light component produced during this sep is given by the Eqs. (26) and (31), and does not depend on the concentration profile. Through the second cycle, the moles of light component produced or consumed at each step is the same as the first cycle even though the concentration profile is different from the first cycle. The moles of light component produced or consumed at the third cycle also will be the same as those at the first cycle. As the cycle number increases, the concentration profiles at the backfill and the co-current depressurization steps will approach cyclic steady state as schematically illustrated in Fig. 4 without the change of the moles of the light component produced or consumed at each step. Thus, we can obtain the performance for this case from the first cycle's operating conditions.

Cases IV and V. These cases are essentially the same as the Cases II and III, respectively, except a complete shock does not form at the end of the high pressure adsorption step since $Y_S > 1$. The two cases are classified depending on whether a complete shock forms at the co-current depressurization step, which is determined by the value of Y_I. The same as the Cases II and III, Y_I could be obtained from Eqs. (22), (24), and (25). If $Y_I > 1$, it corresponds to Case V. The co-current depressurization pressures which ensure a pure light component for Case IV and V are obtained with Eqs. (28) and (29), respectively.

3.5. *Process Performance*

The recovery of light component is defined as

$$R = \frac{N_{HP} + N_{CD} - N_{BF} - N_{PU}}{(1 - y_f) N_H} \tag{32}$$

From Eqs. (12), (14), (17), and (18), N_{PU}, N_{BF}, N_H, N_{HP} are obtained, respectively. The moles of light component produced during the co-current depressurization step, N_{CD}, is given by Eq. (24). N_{CD} is proportional to the pressure difference between the adsorption pressure and co-current depressurization pressure. The co-current depressurization pressure is obtained from Eqs. (29)–(31) depending on the operation condition and determined by the extent of purge and the amount of feed at given values of y_f, β, and Ψ_H. Thus, the recovery of the process could be represented by the extent of purge and amount of feed. Equations (29)–(31) define the relations among the three operating variables, extent of purge, amount of feed and co-current depressurization pressure, at given values of y_f, β, and Ψ_H. Therefore, if two of them are specified, the other one is obtained. As a result, the performance of the process also could be represented by the extent of purge and the co-current depressurization pressure. The advantage of

using the extent of purge and co-current depressurization pressure as independent variables is that they can be used directly in designing or scheduling a multi-bed PSA process. The light component produced during the co-current depressurization step is utilized to repressurize or purge the other column in the multi-bed PSA process. The number of the pressure equalization step and the extent of purge when the effluent of the co-current depressurization step is used to purge the other column, depends on how large quantity of light component from the co-current depressurization step is available. Thus, if one specifies the co-current depressurization pressure, one can decide how many pressure equalization steps can be included and how much quantity of purge gas is available. Moreover, since the number of pressure equalization steps can be performed depends on the number of columns employed, one can decide the number of columns necessary.

The other quantity characterizing the performance of a PSA process is the productivity which is defined as the net amount of light component produced per unit time length. Since the cycle time cannot be implied in an analytical solution, the throughput, T, related to the productivity is defined as the net amount of light component produced per cycle.

$$T = N_{\mathrm{HP}} + N_{\mathrm{CD}} - N_{\mathrm{BF}} - N_{\mathrm{PU}} \tag{33}$$

The productivity is the throughput divided by the cycle time. At this point, the relation between the productivity and the throughput in the multi-bed PSA process should be mentioned. The cycle time is freely set in the single column PSA process, but not in the multi-bed PSA process for the continuous production. If a single column is engaged in the high pressure adsorption step in the multi-bed PSA process, the number of column times the high pressure adsorption step time must be equal to the cycle time for continuous production. The cycle time is the sum of the duration of all the steps constituting the cycle.

$$n_{\mathrm{bed}} \cdot t_{\mathrm{AD}} = t_{\mathrm{cycle}} = t_{\mathrm{AD}} + t_{\mathrm{CD}} + t_{\mathrm{BD}} + t_{\mathrm{PU}} + t_{\mathrm{BF}} \tag{34}$$

If the instantaneous equilibrium is sustained, it is better to keep the cycle time as short as possible in view of the productivity. But, due to flow resistance, the time required to backfill or depressurize the column can't be shortened below a certain time. If we let the minimum time required to execute all the steps except the high pressure adsorption step be t_{min}, the cycle time could be represented as follows

$$t_{\mathrm{cycle}} = \frac{n_{\mathrm{bed}}}{n_{\mathrm{bed}} - 1} t_{\mathrm{min}} \tag{35}$$

Thus, the productivity of the PSA process depends on the number of columns employed. When the number of columns employed is the same between processes, the throughput could be used as an indication of the productivity of each process.

4. Results and discussion

4.1. *Process Performance at Base System (y_f: 0.4, β: 0.1, Ψ_H: 25)*

Figure 5 shows the contour maps of the light component recovery and throughput for the case when the feed composition, y_{f}, is 0.4, β is 0.1, and the pressure ratio, Ψ_{H}, is 25. The extent of purge and co-current depressurization pressure are the independent variables as shown in Fig. 5. X_{min} of this system was 0.01 so that the analysis was performed at $X \geq 0.01$. The critical extent of purge, X_{c}, at which a complete shock first forms at product end at the end of the adsorption step can be found from Eqs. (19) and (21). For this case, X_{c} was 0.49 and this value is the minimum extent of purge above which the prior models can be applied. When the extent of purge, X, is larger than 0.49, a complete shock forms at the high pressure adsorption step if a sufficient amount of feed is introduced ($\alpha > \alpha_{\mathrm{S}}$, Case I). Even if the feed amount introduced is less than α_{S}, a complete shock may form during the co-current depressurization step (Case II). Before mentioned, the Case II happens when one reduces the amount of feed to get more light component at the co-current depressurization step and to diminish the blowdown loss. As shown in Fig. 5(a), the recovery is increased by reducing the co-current depressurization pressure unless the pressure is over reduced. For this system, Case III is not observed. When the extent of purge is large, it is easier for the concentration profile to have a complete shock transition. Comparing Cases II and III to Case IV, the extent of purge of Case IV is smaller than that of Cases II and III. If a complete shock forms at the end of the co-current depressurization step at the lower extent of purge (Case IV), then there always appears a complete shock at the higher extent of purge i.e., Case III never occurs. For both Cases I and II, the recovery has a maximum value at a given extent of purge.

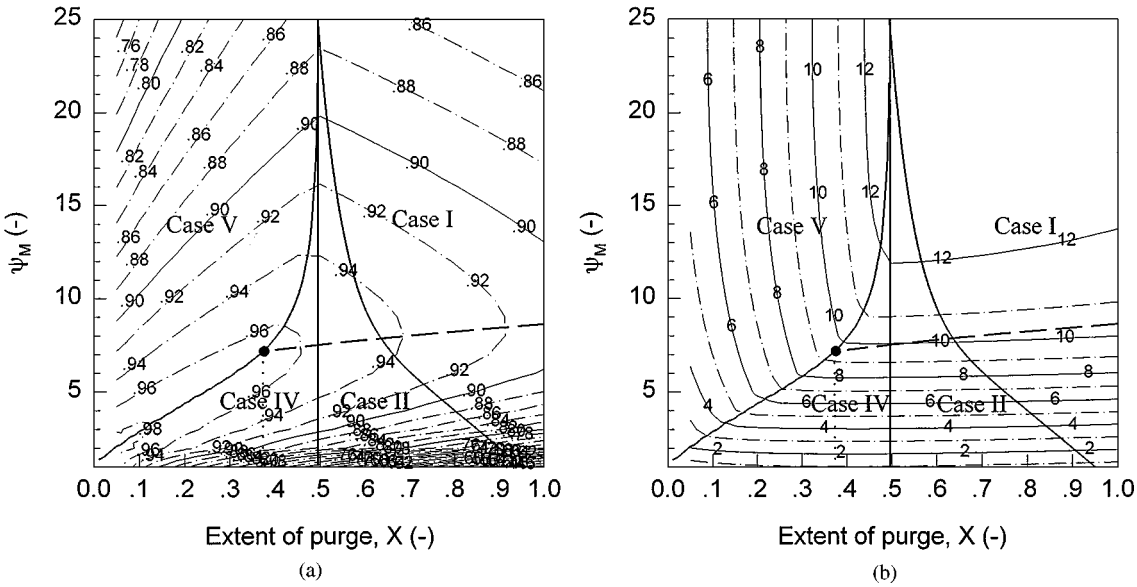

Figure 5. Performance maps for base case (β: 0.1, y_f: 0.4, Ψ_H: 25), (a) recovery, (b) throughput. (●: X_{opt}; —: Optimum co-current depressurization pressure given by Eq. (42)).

When purge extent is less than 0.49, a complete shock never forms during the high pressure adsorption step but may develop during the co-current depressurization step. The upper region at this extent of purge corresponds to the situation that no complete shock appears in the whole cycle (Case V). But, a complete shock appears during the co-current depressurization step at lower region (Case IV). Depending on whether a complete shock forms or not before the blowdown step, the recovery of the process shows a different behavior. When a complete shock forms (Case IV), the recovery shows similar behavior to the Cases I and II. On the other hand, the recovery decreases with the decrease of purge quantity for Case V. In summary, the recovery map can be divided into two regions according to whether a complete shock forms or not before the blowdown step. Crossing over the boundary between Cases I, II, and IV, there is no sharp change in the recovery even though the concentration profile developing at the high pressure adsorption and co-current depressurization steps is different from each other. This is because the concentration profile at the end of the co-current depressurization step develops to a complete shock at all cases.

The recovery could be represented with respect to average composition of the heavy component in waste streams (blowdown and purge effluent). Feed mixture introduced is divided into two streams such as waste and product. From the material balance for the light component, the recovery is represented as follows.

$$R = \frac{(1 - y_f)N_H - (1 - \bar{y}_W)N_W}{(1 - y_f)N_H} \tag{36}$$

where $\bar{y}_W$, N_W is the average composition of the heavy component in the waste stream and moles of waste stream, respectively. Since only the pure light component is assumed as product

$$N_W = \frac{y_f}{\bar{y}_W} N_H \tag{37}$$

Therefore, the recovery is represented as follows

$$R = 1 - \frac{y_f}{1 - y_f}\left(\frac{1}{\bar{y}_W} - 1\right) \tag{38}$$

From Eq. (38), it is clear that the recovery increases as the average composition of heavy component in the waste stream increases. When a complete shock forms before the blowdown step, the total moles leaving the column during the blowdown and purge steps are given, respectively.

$$V_{BD} = \phi[\Psi_M y_M - y_b] + \phi\beta[\Psi_M(1 - y_M) - (1 - y_b)] \tag{39}$$

$$V_{PU} = \phi[y_b - W_A] + \phi[X - \beta(y_b - W_A)] \tag{40}$$

The first terms of two equations represent the moles of the heavy component leaving the column and the second terms represent the moles of the light component. Equations (39) and (40) don't discriminate at which step a complete shock first forms. From Eqs. (38)–(40), the recovery for the Cases I, II, and IV is

$$R = 1 - \frac{y_f}{1 - y_f}\left(\frac{\beta W_A - \beta + X + \beta\Psi_M - \beta\Psi_M y_M}{\Psi_M y_M - W_A}\right) \tag{41}$$

Equation (41) can be applied whenever a complete shock forms before the blowdown step. If the column has a uniform composition of y_b after the blowdown step, the average composition of heavy component of purge effluent is y_b when $X \leq X_{min}$ and then decreases as the purge quantity increases. As a result, the average composition of heavy component of purge effluent is much lower than y_b when the column is completely purged. On the other hand, the composition of the blowdown effluent approaches y_b as the co-current depressurization pressure approaches P_L and decreases with the increase of the co-current depressurization pressure. Thus, at complete purge, the average composition of the heavy component in the waste stream is increased by adding the blowdown effluent when the co-current depressurization pressure is near to P_L. But, since the composition of the heavy component in the blowdown effluent decreases with the increase of Ψ_M, there appears a pressure at which the composition of the heavy component in the blowdown effluent at the pressure is equal to the average composition of the heavy component in the waste stream. Above this pressure, the average composition of the heavy component in the waste stream begins to decrease. This is why an optimum co-current depressurization pressure appears at a given extent of purge. The optimum co-current depressurization pressure could be found from Eq. (41) by putting $\frac{\partial R}{\partial \Psi_M} = 0$

$$(\beta - 1)\frac{(1 - y_M)y_M}{1 + (\beta - 1)y_M}(\beta - X - \beta\Psi_M) + y_M(\beta - X) - \beta W_A = 0 \tag{42}$$

The optimum co-current depressurization pressure with the extent of purge is also shown in Fig. 5(a). As shown in the Fig. 5(a), the optimum co-current depressurization pressure decreases as the extent of purge decreases. It is noted that the optimum co-current depressurization pressure appears at the boundary between the Cases IV and V below X_{opt}.

The throughput is also given in Fig. 5(b). The value on the line represents the dimensionless throughput (T/ϕ). The throughput map is divided into two distinct regions according to whether a complete shock forms or not after the co-current depressurization step. In the region where a complete shock forms before the blowdown step, the throughput almost remains constant along the constant Ψ_M line, however, crossing over the boundary, the throughput begins to decrease. Going along the constant X line in Case V, the throughput almost remains constant. Seeing together the recovery and the throughput maps, the maximum throughput at the fixed recovery or the maximum recovery at fixed throughput appears on the boundary between Cases IV and V. It is also noted that the throughput is almost the same but the recovery becomes high with the decrease of purge quantity along the line representing the optimum co-current depressurization pressure when it is in the region that a complete shock forms before the blowdown step. The recovery is improved slightly by reducing the purge quantity even below X_{opt}, but the throughput decreases rapidly below X_{opt}. Thus, it is better to operate the PSA process at X_{opt} and the corresponding optimum Ψ_M. This implies that the number of pressure equalization steps and the number of columns has a limitation on a highly selective adsorbent.

4.2. *Effect of Adsorbent Selectivity and Feed Composition on Process Performance*

To investigate the effect of adsorbent selectivity, two different values of selectivity were examined. Small value of β means good selectivity by its definition and easy separation of the feed mixture. But, as β decreases, the concentration profile after the purge step gets broader so that the critical extent of purge, $X_c = 0.58$ at $\beta = 0.01$ in Fig. 6, becomes large compared to the base system as shown in Fig. 5. The optimum co-current depressurization pressure is close to the partial pressure of the heavy component in the feed mixture. The change of optimum co-current depressurization pressure with the decrease of the purge quantity in the highly selective adsorbent is smaller than that in a less selective adsorbent. For this highly selective adsorbent, there also appears an extent of purge, X_{opt}, below which the recovery does not change to a great extent while the throughput decreases rapidly. If the extent of purge is reduced exceeding X_{opt}, the optimum co-current depressurization pressure appears on the boundary between a complete shock forming region and non forming region. The effect of co-current

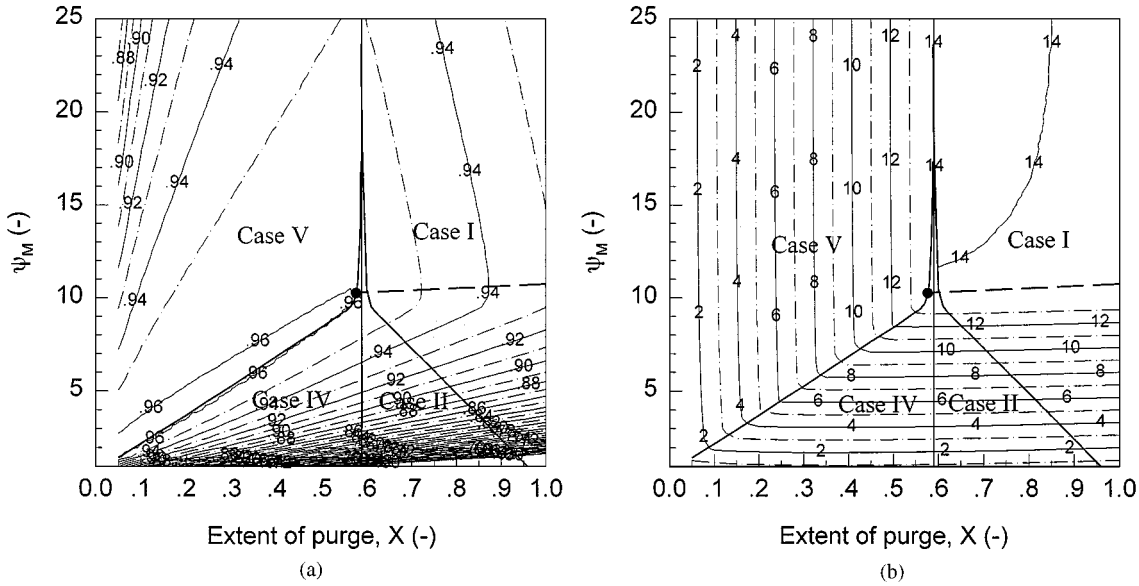

Figure 6. Performance maps for β: 0.01, y_f: 0.4, Ψ_H: 25, (a) recovery, (b) throughput. (●: X_{opt}; —: Optimum co-current depressurization pressure given by Eq. (42)).

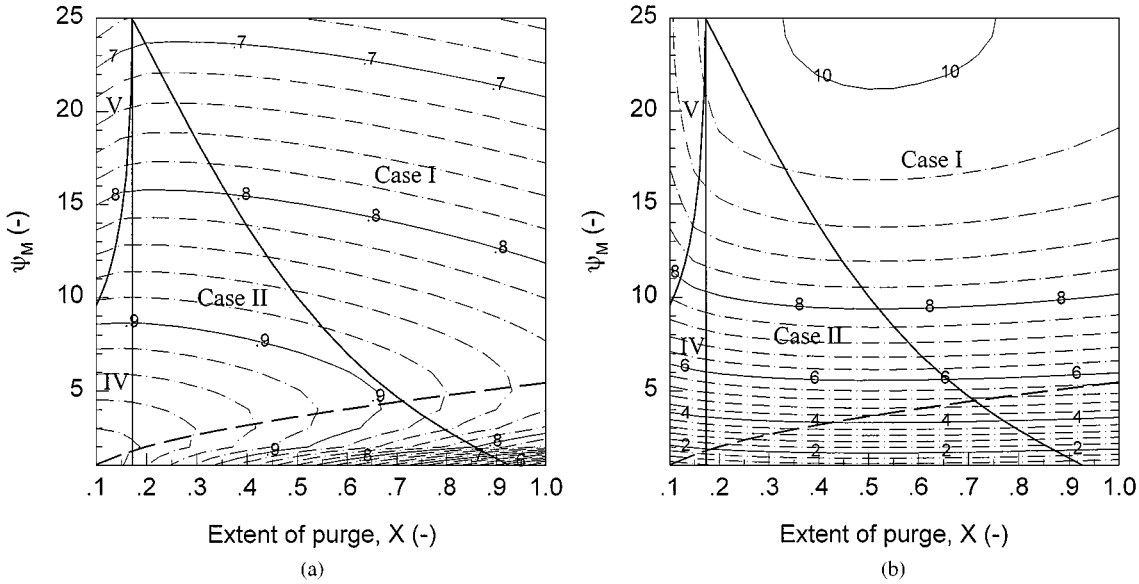

Figure 7. Performance maps for β: 0.3, y_f: 0.4, Ψ_H: 25, (a) recovery, (b) throughput. (—: Optimum co-current depressurization pressure given by Eq. (42)).

depressurization step on the recovery is less significant for a highly selective adsorbent than that for the base system. The increase of the recovery with the co-current depressurization pressure is less than 1% as shown in Fig. 6(a). Thus, as the selectivity increases, a four step process which is operated without the co-current depressurization step can be an alternative to the five step process since it requires less columns and simpler operation. Another merit of the four step process is the large throughput as shown in Fig. 6(b). The largest throughput is obtained when the process is operated without the co-current depressurization step, i.e., at the four step process. The maximum throughput at the fixed recovery appears at the boundary between Case IV and

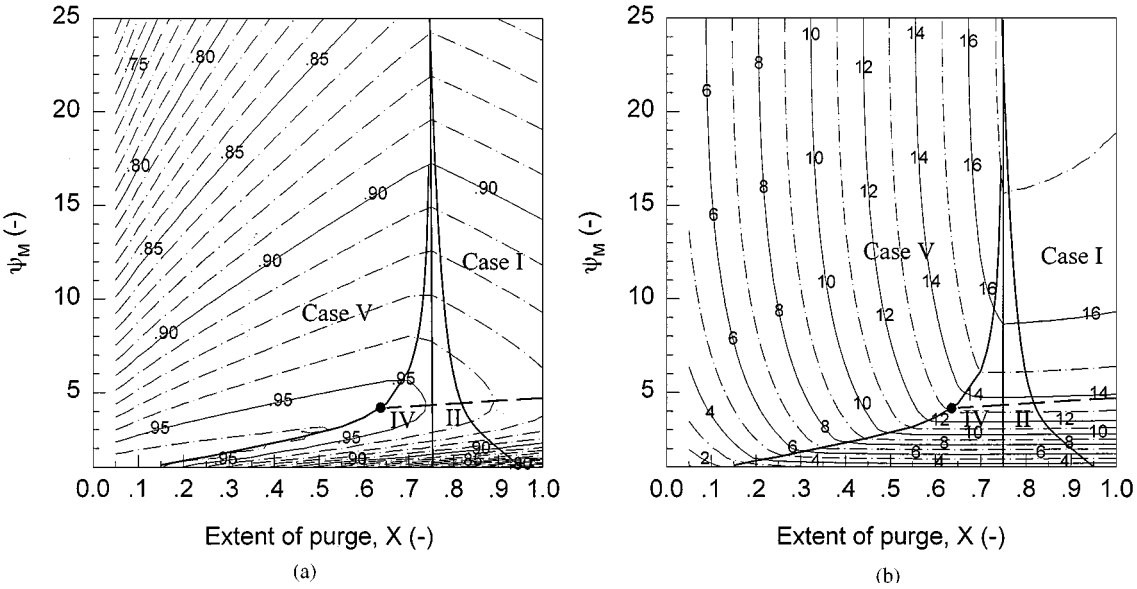

Figure 8. Performance maps for β: 0.1, y_f: 0.2, Ψ_H: 25, (a) recovery, (b) throughput. (●: X_{opt}; —: Optimum co-current depressurization pressure given by Eq. (42)).

Case V like the base system. When β is 0.3, the region where a complete shock forms during adsorption drastically increases as shown in Fig. 7. The optimum co-current depressurization pressure decreases to the lowest system pressure as the purge quantity decreases. As the purge quantity decreases, the optimum recovery increases at the expense of the throughput. But, different from the highly selective adsorbent, there is no extent of purge below which the recovery is improved slightly while the throughput decreases rapidly. The co-current depressurization step takes a more important role in improving the recovery at a less selective adsorbent as shown in Figs. 5–7.

When the feed concentration of the heavy component is lowered, the critical extent of purge increases as shown in Fig. 8. This is because the self-sharpening effect of a concentration profile is not great. Compared to the case that the feed composition of the heavy component is high, the recovery is low but the throughput is high. Like the base system, there is an extent of purge below that the recovery is not improved to a great extent but the throughput decreases rapidly.

5. Conclusion

The performance characteristics of the five-step PSA cycles were analyzed with a equilibrium model assuming isothermal and uncoupled linear isotherms in a broader range of an operational range. Among the steps, the co-current depressurization pressure has its significance in designing the multi-bed PSA process since the number of pressure equalization steps can be executed is determined after the pressure isspecified. Therefore, the process performance was characterized with the purge quantity and co-current depressurization pressure. With the present model, the performance maps from a wide range of operating conditions were obtained. Depending on the operating conditions, the recovery and throughput maps can be divided into two regions: a complete shock forming region and non-forming region before the blowdown step. The throughput at a fixed recovery or the recovery at a fixed throughput have their maximum on the boundary between a complete shock forming region and non-forming region when the selectivity is high. In the region where a complete shock forms, the recovery increases as the purge quantity decreases at constant Ψ_M and has a maximum value at a Ψ_M when the extent of purge is constant. On a highly selective adsorbent, this optimum co-current depressurization pressure is close to the partial pressure of the heavy component in the feed mixture. As the purge quantity decreases, the optimum co-current depressurization pressure decreases. There is an extent of purge below which the recovery is not greatly improved while the throughput decreases rapidly on a highly selective adsorbent. Thus, the number of pressure equalization steps can be performed is restricted on the highly selective adsorbent. When the selectivity is low, a complete shock forms before the blowdown step in almost

all the operating conditions. The optimum co-current depressurization pressure which maximizes the recovery at the constant extent of purge decreases to the lowest system pressure as the purge quantity decreases without much sacrifice of the throughput. The recovery improvement caused by co-current depressurization is much higher in a less selective adsorbent than in a highly selective adsorbent. If the composition of the heavy component in the feed mixture is lowered, the recovery becomes low but the throughput becomes high.

Nomenclature

A	cross section area of the adsorption bed
k_i	Henry's constant for the adsorption of component i
n_{bed}	the number of bed employed in the process
n_i	moles of component i adsorbed per unit column volume
N_{BF}	the amount of light component used to backfill a column from P_{L} to P_{H}
N_{CD}	the amount of light component produced during the co-current depressurization step
N_{H}	the amount of feed mixture introduced to the bed
N_{HP}	the amount of light component produced at high pressure adsorption step
N_{PU}	the amount of light component employed in the purge step
N_{W}	the moles of waste stream
P_{H}	the adsorption pressure
P_i	partial pressure of component i
P_{I}	the pressure where a complete shock first forms at the co-current depressurization step
P_{L}	the lowest column pressure of the cycle
P_{M}	the pressure of the column after co-current depressurization
R	recovery
t	time
t_{AD}	the duration of high pressure adsorption step
t_{BD}	the duration of the blowdown step
t_{BF}	the duration of the backfill step
t_{CD}	the duration of the co-current depressurization step
t_{cycle}	the cycle time
t_{min}	the minimum time required to execute the rest of the steps except the high pressure adsorption step
t_{PU}	the duration of purge step
T	throughput
u	interstitial velocity
V_{BD}	the quantity of gas vented in the blowdown step
V_{PU}	the quantity of gas vented in the purge step
W_{A}	defined in Eq. (13)
X	the extent of purge
X_{c}	the critical extent of purge required so that a complete shock forms first at the product end at the end of the adsorption step.
X_{min}	the minimum extent of purge
X_{opt}	the minimum extent of purge above which the optimum co-current depressurization pressure given by Eq. (42) appears
y	mole fraction of component A in the gas phase
y_{b}	mole fraction of component A in the gas phase after blowdown step
y_{f}	composition of the feed mixture
y_{I}	composition of the gas phase after a complete shock first forms during co-current depressurization step
y_{M}	composition of the gas phase after co-current depressurization step
$\bar{y}_{\text{W}}$	average composition of heavy component in waste stream
Y	the position of a complete shock at the end of high pressure adsorption step
Y_{I}	the position where a complete shock first forms during co-current depressurization step
Y_{S}	the position where a complete shock first forms during high pressure adsorption step
z	distance along the length of the column

Greek Symbols

α	fractional utilization of a bed defined in Eq. (17)
α_{S}	fractional utilization of a bed when a complete shock first forms in the bed
β	$\beta_{\text{A}}/\beta_{\text{B}}$
β_i	$1/[1+(1-\varepsilon)k_i/\varepsilon]$
ε	void fraction of the column
ϕ	$\varepsilon A P_{\text{L}}/RT\beta_{\text{A}}$
Ψ_{H}	$P_{\text{H}}/P_{\text{L}}$
Ψ_{I}	$P_{\text{I}}/P_{\text{L}}$
Ψ_{M}	$P_{\text{M}}/P_{\text{L}}$

References

Bossy, A., D. Tondeur, and A. Jedrzejak, "A Non-Linear Equilibrium Analysis of Blowdown Policy in PSA Separation," *Chem. Engng. J.*, **48**, 173–182 (1992).

Chiang, A.S.T., "Arithmetic of PSA Process Scheduling," *AIChE J.*, **34**, 1910–1915 (1988).

Chiang, A.S.T., "The Cycle Design of an Equilibrium PSA Process," *Proc. AIChE Topical Conf.*, **2**, 262–267 (1995).

Chiang, A.S.T., "An Analytical Solution to Equilibrium PSA Cycles," *Chem. Eng. Sci.*, **51**, 207–216 (1996).

Fernandez, F. and C.N. Kenney, "Model of the PSA Air Separation Process," *Chem. Eng. Sci.*, **38**, 827–834 (1983).

Knaebel, K.S. and F.B. Hill, "PSA: Development of an Equilibrium Theory for Gas Separations," *Chem. Eng. Sci.*, **40**, 2351–2360 (1985).

Matz, M.J. and C.N. Knaebel, "PSA: Effects of Incomplete Purge," *AIChE J.*, **34**, 1486–1492 (1988).

Rousar, I. and P. Ditl, "Pressure Swing Adsorption Analytical Solution for Optimum Purge," *Chem. Eng. Sci.*, **48**, 723–734 (1993).

Shendalam, L.H. and J.E. Mitchell, "A Study of Heatless Adsorption in the Model System CO_2 in He-I," *Chem. Eng. Sci.*, **27**, 1449–1458 (1972).

Suh, S.S. and P.C. Wankat, "Combined Co-current-Countercurrent Blowdown Cycle in Pressure Swing Adsorption," *AIChE J.*, **35**, 523–526 (1989).

Yang, R.T., *Gas Separation by Adsorption Process*, pp. 255–260, Butterworths, Boston, 1987.